High-pressure behavior of $A_2B_2O_7$ pyrochlore (A=Eu, Dy; B=Ti, Zr)

Dylan R. Rittman,[1,a)] Katlyn M. Turner,[1] Sulgiye Park,[1] Antonio F. Fuentes,[2] Jinyuan Yan,[3] Rodney C. Ewing,[1] and Wendy L. Mao[1,4]
[1]*Department of Geological Sciences, Stanford University, Stanford, California 94305, USA*
[2]*Cinvestav Unidad Saltillo, Apartado Postal 663, 25000 Saltillo, Coahuila, Mexico*
[3]*Advanced Light Source, Lawrence Berkeley National Laboratory, Berkeley, California 94720, USA*
[4]*Stanford Institute for Materials and Energy Sciences, SLAC National Accelerator Laboratory, Menlo Park, California 94025, USA*

(Received 12 December 2016; accepted 12 January 2017; published online 24 January 2017)

In situ high-pressure X-ray diffraction and Raman spectroscopy were used to determine the influence of composition on the high-pressure behavior of $A_2B_2O_7$ pyrochlore (A = Eu, Dy; B = Ti, Zr) up to ~50 GPa. Based on X-ray diffraction results, all compositions transformed to the high-pressure cotunnite structure. The B-site cation species had a larger effect on the transition pressure than the A-site cation species, with the onset of the phase transformation occurring at ~41 GPa for B = Ti and ~16 GPa B = Zr. However, the A-site cation affected the kinetics of the phase transformation, with the transformation for compositions with the smaller ionic radii, i.e., A = Dy, proceeding faster than those with a larger ionic radii, i.e., A = Eu. These results were consistent with previous work in which the radius-ratio of the A- and B-site cations determined the energetics of disordering, and compositions with more similarly sized A- and B-site cations had a lower defect formation energy. Raman spectra revealed differences in the degree of short-range order of the different compositions. Due to the large phase fraction of cotunnite at high pressure for B = Zr compositions, Raman modes for cotunnite could be observed, with more modes recorded for A = Eu than A = Dy. These additional modes are attributed to increased short-to-medium range ordering in the initially pyrochlore structured $Eu_2Zr_2O_7$ as compared with the initially defect-fluorite structured $Dy_2Zr_2O_7$.

I. INTRODUCTION

The pyrochlore structure-type, $A_2B_2O_7$, has a wide range of synthetic compositions, over 500, and many important technological applications, including as quantum spin ices,[1] solid oxide fuel cells,[2,3] and nuclear waste forms.[4] The precise species of A- and B-site cations is crucial in all of these applications because of dramatic changes in properties that occur with changes in composition.[5–8]

Most pyrochlore oxide compositions crystallize in one of two closely related structures. The ordered pyrochlore structure (*Fd-3m*) is stable for compositions for which the radius-ratio of the A-site to the B-site cations is greater than 1.46. The cation sub-lattice is face-centered cubic with A- and B-site cations occupying distinct sites—*16c* and *16d*, respectively, as they alternate along the ⟨110⟩ direction. The A-site is coordinated by eight oxygens, while the B-site is coordinated by six oxygens. The anion sub-lattice is a distorted simple cube with 1/8 of the sites vacant. The anion vacancy is on the *8b* site and is tetrahedrally coordinated by four B-site cations. Oxygen occupies the *8a* and *48f* sites, which are tetrahedrally coordinated by four A-site cations and two A- and two B-site cations, respectively. These site labels are based on the origin being at the A-site.[9,10]

When the radius-ratio of the A- and B-site cations is less than 1.46, a disordered, defect fluorite structure (*Fm-3m*) forms. In this structure, the cation species are evenly distributed over both the A- and B-sites, such that there is effectively a single cation site. As such, pyrochlore is essentially a $2 \times 2 \times 2$ superstructure of defect-fluorite due to cation ordering. The cations in defect-fluorite are, on average, seven-coordinated by oxygen due to disordering of the anion vacancies. The anion site is tetrahedrally coordinated by cations.[10]

The behavior of $A_2B_2O_7$ pyrochlore under high pressure has been investigated for a wide variety of compositions.[11–15] However, previous studies have only focused on the effect of changes in cation species on a single site—i.e., only changing the cation on the A-site[12,15] or the B-site.[14] For high pressure studies, this makes comparisons problematic due to differences between experiments, such as the use of different pressure-transmitting media or variations in the maximum pressures attained.

Here, we systematically investigate the effects of changing both the A- and B-site cations on the high-pressure response of rare earth titanate and zirconate pyrochlore with compositions: $Eu_2Ti_2O_7$, $Dy_2Ti_2O_7$, $Eu_2Zr_2O_7$, and $Dy_2Zr_2O_7$. These compositions are referred to as ET ($Eu_2Ti_2O_7$), DT ($Dy_2Ti_2O_7$), EZ ($Eu_2Zr_2O_7$), and DZ ($Dy_2Zr_2O_7$), respectively. Results are consistent with previous studies,[12–21] although by exploring the effects of changing both the A- and B-site cations, we are able to more clearly illustrate the systematic trends in the behavior of pyrochlore at high pressure, including the onset pressure of the phase transformation, the transformation's kinetics, and the short-range coordination of the high-pressure phase.

II. EXPERIMENTAL

$A_2B_2O_7$ (A = Eu, Dy; B = Ti, Zr) samples were synthesized using solid-state methods.[22] Powders of A_2O_3 and BO_2 were mixed in a 1:2 ratio and ball milled for 19 h at room temperature. These powders were then annealed at high temperature for 12 h to eliminate cation anti-site defects and anion Frenkel defects.[22] Samples with B = Ti and Zr were annealed at 1200 °C and 1500 °C, respectively. Compositions with the larger B = Zr cation require higher temperatures to anneal out defects.[23] Instead of simply matching annealing temperatures, we tried to match the *effect* of annealing across compositions. That is, samples were annealed at a temperature that allowed for the maximum number of cation anti-site defects to be eliminated. It is important to recognize that the defect-fluorite structure of DZ is inherently disordered; however, an annealing temperature of 1500 °C was selected to make a consistent comparison to the ordered zirconate pyrochlore. In this case, annealing of DZ caused a decrease in strain.

X-ray diffraction showed that ET ($r_A/r_B = 1.76$), DT ($r_A/r_B = 1.70$), and EZ ($r_A/r_B = 1.48$) synthesized in the pyrochlore structure, while DZ ($r_A/r_B = 1.43$) synthesized in the defect-fluorite structure. These structures are consistent with predictions based on cationic radius-ratio considerations.[4]

Pressure was generated using symmetric diamond anvil cells. Pressure was monitored using the ruby fluorescence method.[24] Uncertainties in pressure, caused by broadening of the fluorescence signal at high pressure, are <1 GPa for pressures below 40 GPa and ~2 GPa for pressures above 40 GPa. Silicone oil was used as the pressure-transmitting medium[25] for all experiments except for Raman spectroscopy of EZ due to the large fluorescence peaks it produced above the sample signal. In this case, a 4:1 methanol:ethanol mixture was used, which produces similar quasi-hydrostatic conditions for the pressure range studied.[26] Comparisons were made to spectra obtained with a silicone oil pressure transmitting medium in order to ensure that this change did not affect the high-pressure behavior—the only differences observed among the samples was the absence of the silicone oil fluorescence peaks.

Non-hydrostatic conditions have been shown to decrease the onset pressure of the phase transformation, though no other significant changes in the character of the X-ray diffraction data were observed.[13] Thus, the choice of pressure transmitting media in this study did not have an adverse effect on our analysis, since it was held constant across experiments.

Samples were studied *in situ* at high pressure using angular dispersive X-ray diffraction and Raman spectroscopy. X-ray diffraction data were collected at beamline 12.2.2 of the Advanced Light Source (ALS), Lawrence Berkeley National Laboratory (LBNL) and at beamline 16 BM-D of the Advanced Photon Source (APS), Argonne National Laboratory (ANL). X-ray energies used were 29.2 keV ($\lambda = 0.4246$ Å) and 40 keV ($\lambda = 0.3100$ Å). Dioptas was used to integrate the two-dimensional diffraction images into diffraction patterns.[27] Maud was used to perform the Rietveld refinement of the diffraction data.[28] Raman spectra were collected with a 514.5 nm laser wavelength and a 10 mW laser power using a Renishaw RM1000 Raman microscope.

III. RESULTS AND DISCUSSION

All samples underwent a pressure-induced phase transformation. The onset of the high-pressure phase is defined as an increase in scattering intensity between the (222) and (004) peaks (Figs. 1 and 2). Computational studies indicate that this is the orthorhombic cotunnite phase (*Pnma*), rather than the compositionally equivalent amorphous or defect-fluorite phase, for all of the titanate and zirconate pyrochlore compounds investigated, and that the cotunnite structure has no site preferences for the different species of cations.[16–18,29] Furthermore, experiments have shown that other fluorite-structured oxides typically transform to cotunnite at high pressure.[30,31] However, in pyrochlore, strain and disorder in the high-pressure phase makes it difficult to conclusively identify the high-pressure as cotunnite in experiments.[14,32]

High-pressure X-ray diffraction patterns of ET and DT are shown in Figs. 1(a) and 1(b), respectively. The onset of the high-pressure phase is approximately equivalent for the

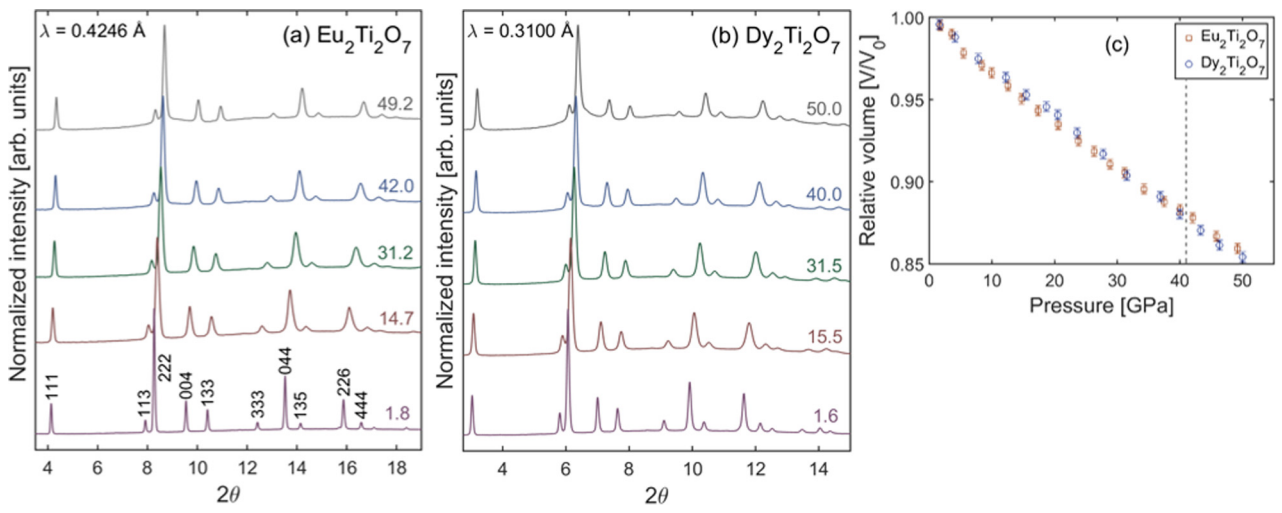

FIG. 1. High pressure X-ray diffraction patterns for (a) ET and (b) DT. Pressures are listed to the right in GPa. (c) Pressure-volume relationships for ET and DT with the phase transformation pressure indicated by a vertical gray dashed line.

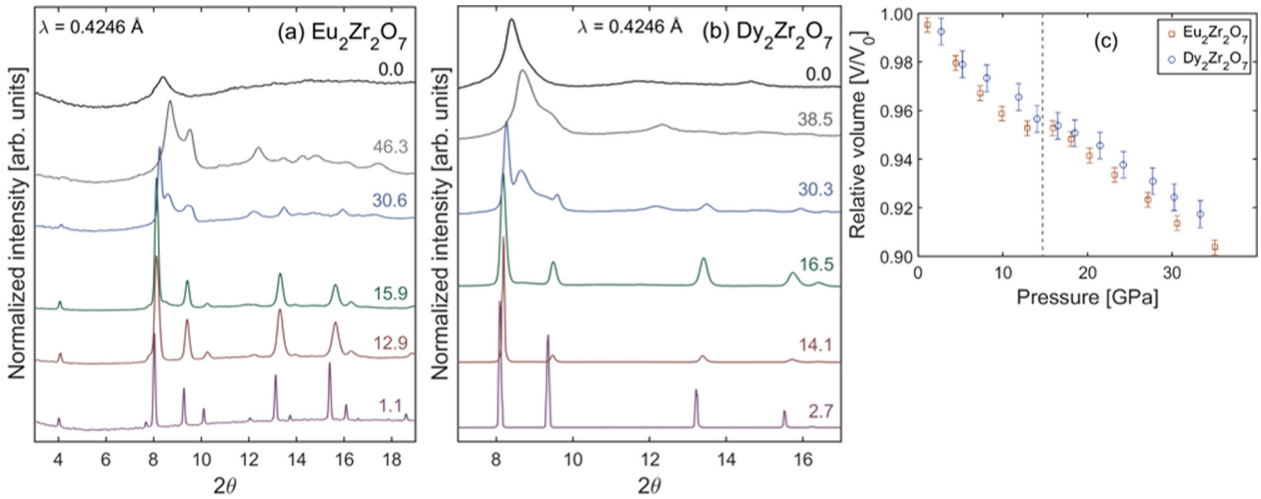

FIG. 2. High pressure X-ray diffraction patterns for (a) EZ and (b) DZ. Pressures are listed to the right in GPa. The top diffraction patterns at 0.0 GPa were taken following decompression from high pressure. (c) Pressure-volume relationship for EZ and DZ with the phase transformation pressure indicated by a vertical gray dashed line.

two samples—42.0 GPa for ET and 40.0 GPa for DT. However, the kinetics of the phase transformation are more rapid for DT than ET. This is indicated by the significantly larger fraction of the high-pressure phase at 50.0 GPa for DT as compared with 49.2 GPa for ET. The pressure-volume relationships for ET and DT, derived from Rietveld refinement of high-pressure X-ray diffraction data, are shown in Fig. 1(c). The rate of compression of both compositions is consistent up to high pressures.

High-pressure X-ray diffraction patterns of EZ and DZ are shown in Figs. 2(a) and 2(b), respectively. The onset of the high-pressure phase is approximately equivalent for the two samples—15.9 GPa for EZ and 16.5 GPa for DZ. However, the kinetics of the phase transformation is faster for DZ than EZ. The transformation is complete by 46.3 GPa in EZ and by 38.5 GPa in DZ. This behavior is consistent with the results for the comparison between ET and DT (Fig. 1), where the transformation proceeds more quickly for compositions with the smaller Dy A-site cation. The pressure-volume relationships for EZ and DZ, derived from Rietveld refinement of high-pressure X-ray diffraction data, are shown in Fig. 2(c). A "kink" exists in the data for both zirconate compositions in the region of ∼15–20 GPa, where there is a marked decrease in the rate of compression. This "kink" has been previously ascribed to structural relaxation caused by the onset of the cotunnite phase,[32] consistent with the data shown here. Compositions with B = Ti have a low phase fraction of cotunnite at the highest pressure studied (∼50 GPa), and thus do not show this anomaly (Fig. 1(c)).

Diffraction data collected upon quenching to ambient pressure is provided for DZ and EZ (Figs. 2(a) and 2(b)). DZ transitions from cotunnite to a different phase upon decompression, likely the X-phase that has been previously observed in pyrochlore quenched from high pressure.[33] The diffraction of quenched EZ appears amorphous, though the positions of the diffraction maxima are consistent with the X-phase. Thus, it is also possible that $Eu_2Zr_2O_7$ quenches to an X-phase structure with large amounts of strain. The failure to recover the cotunnite phase to ambient pressure is consistent with previous experimental studies[13,14] and computational work regarding its dynamical stability.[34]

The cationic radius-ratio can be used to predict the high-pressure behavior of pyrochlore and related structure types. A larger radius-ratio leads to a higher defect formation energy,[19–21] which causes higher resistance to disordering under pressure. The energy to form these anion Frenkel-pairs in ET, DT, EZ, and DZ are approximately 2, 1, −0.4, and −1 eV, respectively.[19] Formation energies for cation antisite defects in ET, DT, EZ, and DZ are approximately 2, 2, 1.75, and 0.75 eV, respectively.[19] The trend in these formation energies correlates well with the relative resistance of the various compositions to structural transformation upon compression, with higher defect formation energies requiring a higher pressure to induce a phase transformation.

Changing the B-site cation (Ti *vs.* Zr) affects the cationic radius-ratio (and, thus, the defect formation energy) more than changing the A-site cation (Eu vs. Dy).[19–21] As such, the titanate compositions behave more similarly than the equivalent zirconate compositions. This is evidenced by the large difference in the fraction of cotunnite phase observed at the highest pressures reached for ET and DT (Fig. 1) as compared with both EZ and DZ (Fig. 2), as well as the different onset pressure of the transformation in titanates *vs.* zirconates. The larger defect formation energy in titanates as compared with zirconates means titanates require a higher pressure to transform to the high-pressure phase.[15] We note that this comparison of the effects of A-site *vs.* B-site cations does not necessarily extend to other B-site compositions since, for example, B = Zr *vs.* B = Hf would have a very similar ionic radii and therefore have a very similar behavior based on the cationic radius ratio principle.

Although the B-site cation has a larger effect on the high-pressure behavior of pyrochlore, the A-site cation also influences the phase transformation. Computational studies indicate that the transition pressures of EZ and DZ should be below 18 GPa, with the transition pressure of EZ being ∼2 GPa higher than DZ due to the larger A-site cation in EZ.[17] In our experiments, we find that both the EZ and DZ

transition pressures were indeed below 18 GPa. However, the transition pressure of EZ is slightly higher than that of DZ (Fig. 2). The difference in transition pressure (0.6 GPa) is not significant and may be explained by differences in sample loading conditions in the diamond anvil cell[35] and/or by slightly overshooting the onset of the transition when increasing pressure during the experiment. The effect of the A-site cation can be more readily observed in the kinetics of the phase transformation, where kinetics are more rapid for A = Dy than A = Eu (Figs. 1 and 2). Since the transformation to cotunnite is kinetically inhibited by the disordering of cations,[17] the lower cationic radius-ratio of Dy as compared with Eu allows the transformation to proceed more quickly because its cation anti-site defect energy is lower.[20]

While X-ray diffraction provides information on the onset and kinetics of the phase transformation, Raman spectroscopy provides additional detail on the short-range order of both the low- and high-pressure phases. High-pressure Raman spectra of ET and DT are shown in Figs. 3(a) and 3(b), respectively. The behavior of ET and DT are very similar, with a loss of all Raman modes from ordered pyrochlore at slightly above ~50 GPa, a pressure at which the X-ray diffraction data still show a large fraction of the ordered pyrochlore (Fig. 1). Thus, the loss of fully-ordered pyrochlore Raman modes is due to distortions of the coordination polyhedral rather than rearrangement of cations. This is supported by the growth of the broad mode at $\omega = 800\,\mathrm{cm}^{-1}$ at high pressure, which has been previously attributed to distortions to the oxygen positions of the BO_6 octahedra.[12,36]

High-pressure Raman spectra of EZ and DZ are shown in Figs. 4(a) and 4(b), respectively. Spectra recorded at low pressure show more ordering in EZ than in DZ, as evidenced by its better defined peaks.[37–39] This is due to the ordered pyrochlore structure of EZ compared with the disordered defect-fluorite structure of DZ. However, DZ still retains some local ordering as evidenced by its broad peaks that are consistent with the EZ spectra. This may be related to short-to-medium range ordering that exists even in defect-fluorite structured $A_2B_2O_7$ compounds.[40] Furthermore, the radius-ratio of DZ puts it just below the threshold for cation ordering into the pyrochlore phase,[10] so it is possible that some short-range order is retained.

The Raman modes from the ordered pyrochlore phase are still observed at the highest pressure reached for EZ, 49.3 GPa, while the modes in DZ are indistinguishable by 22.4 GPa, at which point the spectra resemble a true defect-fluorite.[38,41] Raman modes attributed to the high-pressure cotunnite phase are marked by black circles in Fig. 4 at the pressure they first appear—34.2 GPa for EZ and 25.1 GPa for DZ. These high-pressure modes occur well above the onset of the formation of the high-pressure phase, as evidenced by X-ray diffraction. The high-pressure cotunnite Raman mode at $\sim 550\,\mathrm{cm}^{-1}$ has been previously observed in compressed $Gd_2Zr_2O_7$ and $Sm_2Zr_2O_7$.[13,32] Additional high-pressure Raman modes at $< 350\,\mathrm{cm}^{-1}$ are observed to emerge in EZ along with the mode at $\sim 550\,\mathrm{cm}^{-1}$. This suggests that these lower wavenumber modes also originate from the cotunnite phase. These modes have not been previously reported in two-cation pyrochlores. However, similar modes have been observed in the high-pressure cotunnite phase of the single-cation CeO_2, which is fluorite-structured at ambient conditions.[42]

The atomistic mechanism for high-pressure disordering in pyrochlore differs slightly between zirconates and titanates, though both have the formation of anion Frenkel pairs precede cation disordering. For compositions with B = Zr, Rietveld refinement of high-pressure X-ray diffraction data has shown that changes to the anion sub-lattice occur prior to the generation of anti-site defects, and this has been further substantiated by high-pressure Raman spectroscopy data.[43] The generation of anion Frenkel-pairs makes the pyrochlore cation sites, originally differentiated by coordination scheme (6-fold vs. 8-fold), more similar by trending towards a uniform 7-fold coordination. This more uniform coordination scheme across lattice sites lessens the energetic preference for a specific cation to reside on a specific site, thus promoting the generation of cation anti-site defects.

For compositions with B = Ti, loss of all pyrochlore ordered Raman modes occurs while the X-ray diffraction data still show an ordered pyrochlore structure. This has been observed in previous studies,[12,44] and has also been observed here (Figs. 1 and 3). Since X-ray diffraction is sensitive to

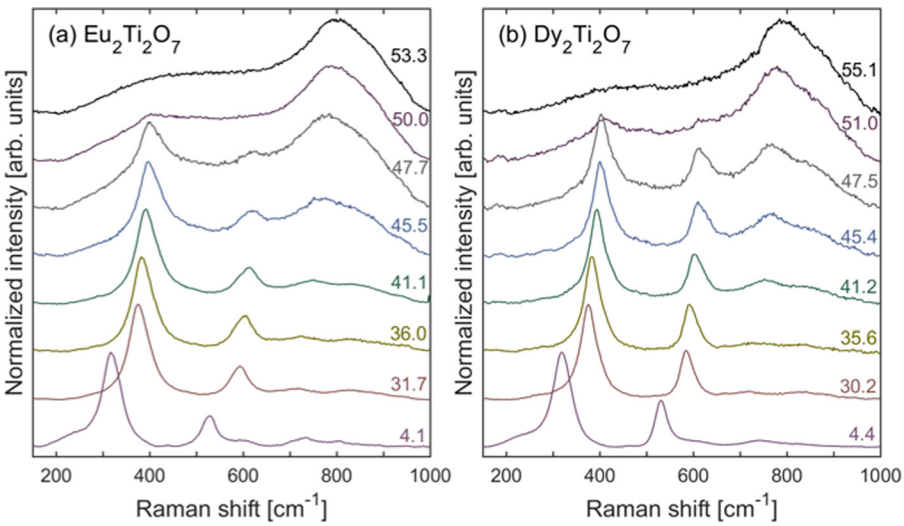

FIG. 3. High pressure Raman spectra for (a) ET and (b) DT. Pressures are listed to the right in GPa.

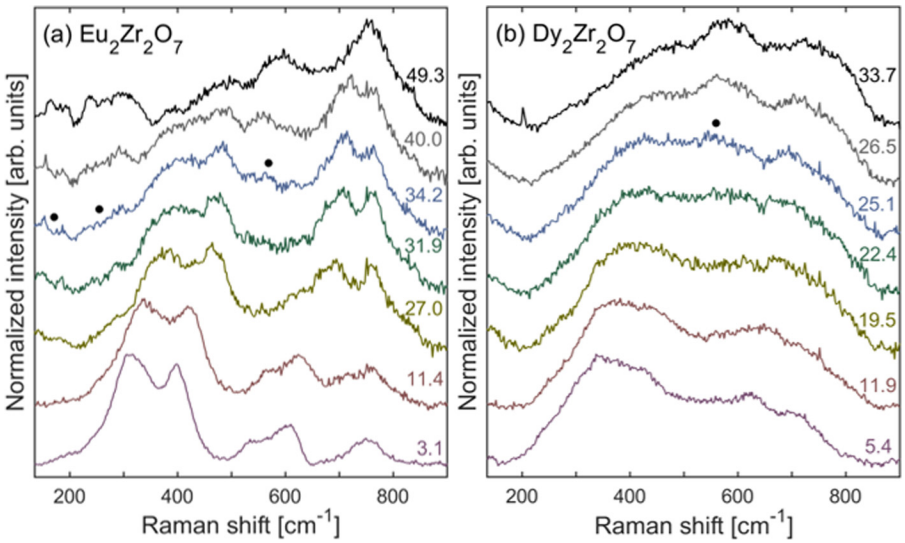

FIG. 4. High pressure Raman spectra for (a) EZ and (b) DZ. Modes attributed to the high-pressure cotunnite phase are marked by black circles at the lowest pressure at which they first appear. Pressures are listed to the right in GPa.

periodic cation positioning while Raman spectroscopy is sensitive to local coordination between cations and anions, this shows that anion disorder precedes cation disordering. While Zr^{4+} has a similar ionic radius compared to the rare-earths that occupy the A-site, Ti^{4+} has a much smaller radius. This makes it more likely that the coordination of Ti stays at six even after disordering.[45] Thus, the disordering of the anion sublattice is better described by a distortion of the TiO_6 octahedra.[12,44]

IV. CONCLUSION

In summary, we have analyzed the effects of composition on the high-pressure response of $A_2B_2O_7$ pyrochlore by isolating changes in composition at the A- and B-sites. Overall, the cationic radius-ratio can be used to predict the response to high pressure, as it also determines the defect formation energy. For the compositions studied here, changes in the B-site cation had a greater effect on material behavior since it had a larger effect on the radius-ratio. The pyrochlore-to-cotunnite transition pressure is ~41 GPa for B = Ti and ~16 GPa for B = Zr. Changes in the A-site cation affect the kinetics of the high-pressure phase transformation, with the transformation proceeding more quickly for compositions with a smaller cationic radius-ratio (*i.e.*, A = Dy is faster than A = Eu).

Raman spectra for B = Ti showed a complete disordering of the anion sub-lattice while X-ray diffraction showed that the sample was still mostly an ordered pyrochlore. The lower transition pressure of B = Zr samples allowed cotunnite Raman modes to be identified. Raman modes of the cotunnite phase not previously reported were observed in the low wavenumber ($<350\,cm^{-1}$) regime for EZ, but not DZ. These additional modes are attributed to increased short-to-medium range ordering that may persist in the cotunnite phase of the initially pyrochlore structured EZ, but not the initially defect-fluorite structured DZ.

ACKNOWLEDGMENTS

This work was supported as part of "Materials Science of Actinides," an Energy Frontier Research Center funded by the U.S. Department of Energy (DOE) Office of Science, Basic Energy Sciences (Grant No. DE-SC0001089). X-ray diffraction data were collected at beamlines HPCAT (Sector 16), APS, ANL, and 12.2.2, ALS, LBNL. HPCAT operations are supported by DOE-NNSA under Award No. DE-NA0001974 and DOE-BES under Award No. DE-FG02-99ER45775, with partial instrumentation funding by NSF. The APS is a U.S. DOE Office of Science User Facility operated for the DOE Office of Science by ANL under Contract No. DE-AC02-06CH11357. The ALS is supported by the Director, Office of Science, Office of Basic Energy Sciences, of the U.S. DOE under Contract No. DE-AC02-05CH11231. Travel was partially supported by the McGee Research Grant program through Stanford University.

[1]D. J. Morris, D. A. Tennant, S. A. Grigera, B. Klemke, C. Castelnovo, R. Moessner, C. Czternasty, M. Meissner, K. C. Rule, J. U. Hoffmann, and K. Kiefer, Science **326**, 411 (2009).
[2]M. Pirzada, R. W. Grimes, L. Minervini, J. F. Maguire, and K. E. Sickafus, Solid State Ionics **140**, 201 (2001).
[3]B. J. Wuensch, K. W. Eberman, C. Heremans, E. M. Ku, P. Onnerud, E. M. Yeo, S. M. Haile, J. K. Stalick, and J. D. Jorgensen, Solid State Ionics **129**, 111 (2000).
[4]R. C. Ewing, W. J. Weber, and J. Lian, J. Appl. Phys. **95**, 5949 (2004).
[5]J. A. Díaz-Guillén, M. R. Díaz-Guillén, K. P. Padmasree, A. F. Fuentes, J. Santamaría, and C. León, Solid State Ionics **179**, 2160 (2008).
[6]J. Lian, J. Chen, L. M. Wang, R. C. Ewing, J. M. Farmer, L. A. Boatner, and K. B. Helean, Phys. Rev. B **68**, 134107 (2003).
[7]K. J. Moreno, G. Mendoza-Suárez, A. F. Fuentes, J. García-Barriocanal, C. León, and J. Santamaria, Phys. Rev. B **71**, 132301 (2005).
[8]J. Snyder, B. G. Ueland, A. Mizel, J. S. Slusky, H. Karunadasa, R. J. Cava, and P. Schiffer, Phys. Rev. B **70**, 184431 (2004).
[9]B. C. Chakoumakos, J. Solid State Chem. **53**, 120 (1984).
[10]M. A. Subramanian, G. Aravamudan, and G. V. Subba Rao, Prog. Solid State Chem. **15**, 55 (1983).
[11]S. Saha, D. V. Muthu, C. Pascanut, N. Dragoe, R. Suryanarayanan, G. Dhalenne, A. Revcolevschi, S. Karmakar, S. M. Sharma, and A. K. Sood, Phys. Rev. B **74**, 064109 (2006).
[12]F. X. Zhang and S. K. Saxena, Chem. Phys. Lett. **413**, 248 (2005).
[13]F. X. Zhang, J. Lian, U. Becker, R. C. Ewing, J. Hu, and S. K. Saxena, Phys. Rev. B **76**, 214104 (2007).
[14]F. X. Zhang, M. Lang, U. Becker, R. C. Ewing, and J. Lian, Appl. Phys. Lett. **92**, 011909 (2008).
[15]F. X. Zhang, J. W. Wang, J. Lian, M. K. Lang, U. Becker, and R. C. Ewing, Phys. Rev. Lett. **100**, 045503 (2008).
[16]H. Y. Xiao, F. Gao, and W. J. Weber, Phys. Rev. B **80**, 212102 (2009).

[17]H. Y. Xiao, F. X. Zhang, F. Gao, M. Lang, R. C. Ewing, and W. J. Weber, Phys. Chem. Chem. Phys. **12**, 12472 (2010).
[18]H. Y. Xiao and W. J. Weber, J. Phys.: Condens. Matter **23**, 035501 (2011).
[19]Y. Li, P. M. Kowalski, G. Beridze, A. R. Birnie, S. Finkeldei, and D. Bosbach, Scr. Mater. **107**, 18 (2015).
[20]L. Minervini, R. W. Grimes, and K. E. Sickafus, J. Am. Ceram. Soc. **83**, 1873 (2000).
[21]K. E. Sickafus, L. Minervini, R. W. Grimes, J. A. Valdez, M. Ishimaru, F. Li, K. J. McClellan, and T. Hartmann, Science **289**, 748 (2000).
[22]A. F. Fuentes, K. Boulahya, M. Maczka, J. Hanuza, and U. Amador, Solid State Sci. **7**, 343 (2005).
[23]K. J. Moreno, A. F. Fuentes, U. Amador, J. Santamaria, and C. Leon, J. Non-Cryst. Solids **353**, 3947 (2007).
[24]H. K. Mao, J. A. Xu, and P. M. Bell, J. Geophys. Res.: Solid Earth **91**, 4673, doi:10.1029/JB091iB05p04673 (1986).
[25]D. D. Ragan, D. R. Clarke, and D. Schiferl, Rev. Sci. Instrum. **67**, 494 (1996).
[26]S. Klotz, J. C. Chervin, P. Munsch, and G. Le Marchand, J. Phys. D: Appl. Phys. **42**, 075413 (2009).
[27]C. Prescher and V. B. Prakapenka, High Pressure Res. **35**, 223 (2015).
[28]L. Lutterotti, S. Matthies, and H. R. Wenk, *IUCr: Newsletter of the CPD* (International Union of Crystallography, 1999), Vol. 21, p. 14.
[29]G. Catillon and A. Chartier, J. Appl. Phys. **116**, 193502 (2014).
[30]S. J. Duclos, Y. K. Vohra, A. L. Ruoff, A. Jayaraman, and G. P. Espinosa, Phys. Rev. B **38**, 7755 (1988).
[31]M. Idiri, T. Le Bihan, S. Heathman, and J. Rebizant, Phys. Rev. B **70**, 014113 (2004).
[32]F. X. Zhang, J. Lian, U. Becker, L. M. Wang, J. Hu, S. Saxena, and R. C. Ewing, Chem. Phys. Lett. **441**, 216 (2007).
[33]M. Lang, F. X. Zhang, J. Zhang, J. Wang, B. Schuster, C. Trautmann, R. Neumann, U. Becker, and R. C. Ewing, Nat. Mater. **8**, 793 (2009).
[34]B. T. Wang, P. Zhang, R. Lizarraga, I. Di Marco, and O. Eriksson, Phys. Rev. B **88**, 104107 (2013).
[35]F. X. Zhang, M. Lang, and R. C. Ewing, Appl. Phys. Lett. **106**, 191902 (2015).
[36]M. T. Vandenborre, E. Husson, J. P. Chatry, and D. Michel, J. Raman Spectrosc. **14**, 63 (1983).
[37]M. Glerup, O. F. Nielsen, and F. W. Poulsen, J. Solid State Chem. **160**, 25 (2001).
[38]B. P. Mandal, N. Garg, S. M. Sharma, and A. K. Tyagi, J. Solid State Chem. **179**, 1990 (2006).
[39]B. P. Mandal, P. S. R. Krishna, and A. K. Tyagi, J. Solid State Chem. **183**, 41 (2010).
[40]J. Shamblin, M. Feygenson, J. Neuefeind, C. L. Tracy, F. Zhang, S. Finkeldei, D. Bosbach, H. Zhou, R. C. Ewing, and M. Lang, Nat. Mater. **15**, 507 (2016).
[41]B. E. Scheetz and W. B. White, J. Am. Ceram. Soc. **62**, 468 (1979).
[42]G. A. Kourouklis, A. Jayaraman, and G. P. Espinosa, Phys. Rev. B **37**, 4250 (1988).
[43]F. X. Zhang, M. Lang, Z. Liu, and R. C. Ewing, Phys. Rev. Lett. **105**, 015503 (2010).
[44]F. X. Zhang, B. Manoun, and S. K. Saxena, Mater. Lett. **60**, 2773 (2006).
[45]M. L. Sanjuan, C. Guglieri, S. Diaz-Moreno, G. Aquilanti, A. F. Fuentes, L. Olivi, and J. Chaboy, Phys. Rev. B **84**, 104207 (2011).